

# BENCHMARKING AND EXPLORING PARAMETER SPACE OF THE 2-PHASE BUBBLE TRACKING MODEL FOR LIQUID MERCURY TARGET SIMULATION\*

L. Lin<sup>†</sup>, H. Tran, M. I. Radaideh, D. Winder  
Oak Ridge National Laboratory, Oak Ridge, TN, USA

## Abstract

High intensity proton pulses strike the Spallation Neutron Source (SNS)'s mercury target to provide bright neutron beams. These strikes also deposit extensive energy into the mercury and its steel vessel. Prediction of the resultant loading on the target is difficult when helium gas is intentionally injected into the mercury to reduce the loading and to mitigate the pitting damage on the vessel. A 2-phase material model that incorporates the Rayleigh-Plesset (R-P) model is expected to address this complex multi-physics dynamics problem by including the bubble dynamics in the liquid mercury. We present a benchmarking study comparing the measured target strains in the SNS target station with the simulation results of the solid mechanics simulation framework. We investigate a wide range of various physical model parameters, including the number of bubble families, bubble size distribution, viscosity, surface tension, etc. to understand their impact on simulation accuracy. Our initial findings reveal that using 8-10 bubble families in the model renders a simulation strain envelope that covers the experimental ones. Further optimization studies are planned to predict the strain response more accurately.

## INTRODUCTION

The spallation reaction at the Spallation Neutron Source (SNS) at Oak Ridge National Laboratory involves an intense proton pulse hitting a mercury target to produce the most intense pulsed neutron beams in the world for scientific and materials discovery [1]. Unfortunately, the first target station at the SNS experienced frequent premature failures due to fatigue damage and pitting damage on the target's internal walls caused by the mercury cavitation [2,3]. Long-term diagnostics are very difficult because in-place devices will be damaged by the high radiation around the target in a very short time. Due to the absence of long-term diagnostics, high-fidelity modeling and simulation become important tools to facilitate the target's fatigue analysis and to improve the target's design [4]. The values of digital twins

of the mercury target have already been demonstrated by using ABAQUS [5]. However, a discrepancy between the simulated and measured strain has always been observed, especially when helium gas is intentionally injected into the mercury to reduce pitting damage [2, 6].

The injected helium bubbles in the mercury flow can significantly reduce the pitting damage on the vessel's internal wall and reduce the strain of the surrounding vessel [7–10]. The additional gas phase introduced by the helium bubbles also converts the mercury fluid into a fluid-bubble mixture. A 2-phase model that incorporates the Rayleigh-Plesset (R-P) model for the gas phase was developed [11] to incorporate the helium bubbles' dynamic behavior with liquid mercury. For convenience, the 2-phase model will be referred to hereafter as the R-P model. As for the R-P model itself, several physical parameters, such as bubble sizes and their group distribution, are still difficult to measure directly. More calibration methods are needed to inversely identify these physical parameters, or their ranges if possible. Therefore, improvement of this bubbly mercury model to predict the target vessel's dynamic stress/strain under pulsed loads within a reliable confidence range, becomes important for the design of current and future targets.

By leveraging the measured strain data for the target with helium bubbles injected, this research work investigates a wide range of various physical model parameters including the number of bubble families, bubble size distribution, viscosity, surface tension, and others to know their impact on simulation results. Our initial findings are reported in the following sections.

## METHODS

The R-P model was developed to include bubble dynamics in liquid mercury contained in a flexible structure. However, the model itself relies on uncertain physics parameters that cannot be readily determined for the SNS target, and therefore must be calibrated with experimental measurement. Direct measurement or observation within the vessel turned out to be extremely difficult [3]. Instead, strain gauges attached on the vessel's external surface [2] have been successfully applied to monitor target's dynamic response. Figure 1 shows some of the sensor locations on the stainless steel vessel's external surface. The strong (23.3 kJ) but short (0.7  $\mu$ s) proton pulses result in stress/strain waves propagating to the stainless-steel vessel, which can be measured through the attached sensors. Measurements of the sensor strains for 2 milliseconds after the pulse delivery under the same pulse power level (1.4 MW) but different loading cycles have been

\* This work was supported by the DOE Office of Science under grant DE-SC0009915 (Office of Basic Energy Sciences, Scientific User Facilities program). The authors like to thank Hao Jiang from ORNL for her suggestions to improve this paper. This research used resources of the Computer and Data Environment for Science (CADES) at the Oak Ridge National Laboratory, which is supported by the Office of Science of the U.S. Department of Energy under Contract No. DE-AC05-00OR22725. This manuscript has been authored by UT-Battelle, LLC, under contract DE-AC05-00OR22725 and DE-AC05-76RL0-1830 with the US Department of Energy (DOE).

<sup>†</sup> linl@ornl.gov

collected and processed as the baseline for validating the target model simulations.

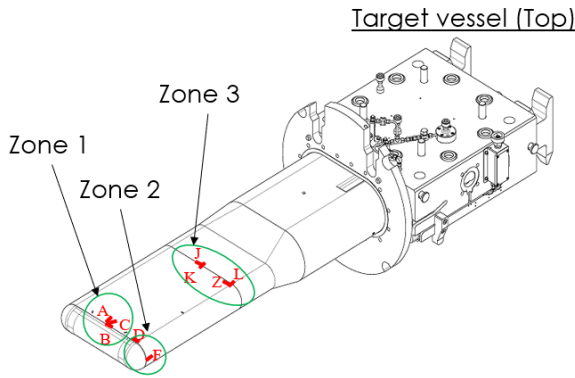


Figure 1: Target vessel and the sensor locations.

The basic form of the Rayleigh–Plesset equation can be expressed as [11, 12]:

$$R\ddot{R} = -\frac{3}{2}\dot{R}^2 + \frac{1}{\rho L_0} [p_{b0}(\frac{R_0}{R})^{3\gamma} - 4\mu\frac{\dot{R}}{R} - \frac{2\sigma}{R} - p_{b0} - p], \quad (1)$$

in which  $R$  is the radius of the bubble,  $\dot{R}$  is the time rate of change of the radius of the bubble, and  $\ddot{R}$  is the time rate of change of  $\dot{R}$ ,  $\rho$  is the density of the fluid surrounding the bubble,  $\mu$  is the kinematic viscosity of the surrounding fluid,  $\gamma$  is the adiabatic index of the bubble gas,  $\sigma$  is the surface tension of the fluid,  $p_{b0}$  is the initial pressure of the bubble but is used in the R-P model as the pressure in the surrounding fluid that contains many bubbles. By simultaneously solving the coupled equations for an arbitrary number of bubble families and the surrounding compressible liquid to conserve pressure and strain, the time-varying bubble radii and their derivatives can be numerically solved. Each bubble family represents the number of bubbles per initial volume that start at the same equilibrium size. Using an arbitrary number of bubble families allows an actual distribution of bubble sizes and densities to be approximated. The bubbly model used in this approach considers only incondensable helium gas bubbles, and mercury vapor bubbles are not explicitly modeled in this approach [11].

With this governing approach, the dynamics of the mixture can be integrated into a customized material subroutine in the Sierra finite element code. However, the real gas bubble distributions are still unknown or difficult to observe within the steel vessel. Inverse machine learning method could help optimize some key parameters in the mercury material model [13], but may also be inefficient or lead to unsatisfactory model prediction if the method is applied in physically invalid parameters space. To tackle this issue, this work investigates a wide range of various physical model parameters, including the bubble size distribution, the number of bubble families, mercury kinematic viscosity, mercury surface tension, helium adiabatic index, and mercury bulk modulus. A limited number of full target simulations were

performed with these varying model parameters to further understand their impact on the bubbly mercury target system.

## RESULTS

### Effect of Bubble Distribution

We investigate the sensitivity of the strain response in the R-P model with respect to the bubble distribution and the number of bubble families. Here, the four physical parameters are fixed at their nominal value, e.g., bulk modulus  $K = 2.86e+10$  Pa, surface tension  $\sigma = 0.47$  N/m, adiabatic index  $\gamma = 1.66$ , and viscosity  $\mu = 0.0015$  N-s/m<sup>2</sup>. Our preliminary study shows that right-skewed distributions (i.e., with mass concentrated on the small bubble size) are more promising to capture the ground truth distribution of the bubbles. Several other distribution shapes were investigated but are not reported here due to space limitation and un-satisfactory results. Hence, we choose two right-skewed distributions with different skewness to illustrate the results. Their corresponding cumulative distribution functions (CDF) are shown in Fig. 2. We use 7 different sets of bubble families to approximate each distribution, with the number of families ranging from 3 to 15.

Figure 3 reveals that the sensor A strain response is sensitive to the number of bubble families used to approximate a bubble distribution. Generally, more families result in higher peaks. A comparison across the left and right plots shows that the strain responses from large number of families (10 or 15 members) are less sensitive to the form of the CDF curves than those from smaller number of families. From this angle, moderate or large number of families are more advantageous (however, they also require higher computational cost).

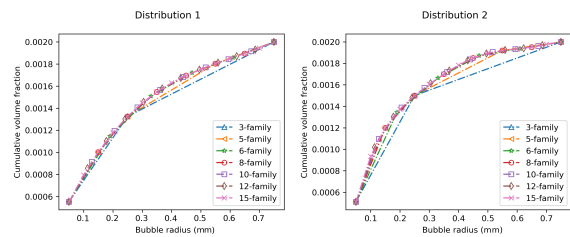


Figure 2: The bubble distributions and their approximations using different sets of bubble families.

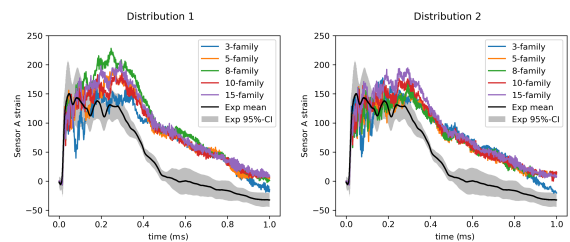


Figure 3: Effect of the bubble distributions and number of families on the sensor A strain.

## Effect of Physical Model Parameters

We investigate the sensitivity of four physical parameters  $K$ ,  $\sigma$ ,  $\gamma$ ,  $\mu$  on the strain response in the R-P model. The bubble distribution is fixed to Distribution 1 (Fig. 2, left) with 8 bubble families, given that this distribution shows a better agreement to the experimental data. Figure 4 shows the effect of changing the parameters on the selected sensor (A) over a wide range of interest. The variations were evaluated by varying one parameter while fixing the other three at their nominal values.

The results clearly show that sensor A strain response is very sensitive to changes in the mercury bulk modulus, typically with lower modulus leading to higher strain response. This sensitivity of the modulus is expected due to the change in the density and/or speed of sound of mercury, which have been observed before for the simple equation of state (EOS) simulations [13, 14]. The other three physical parameters have negligible impact on the strain response despite significant changes in their values.

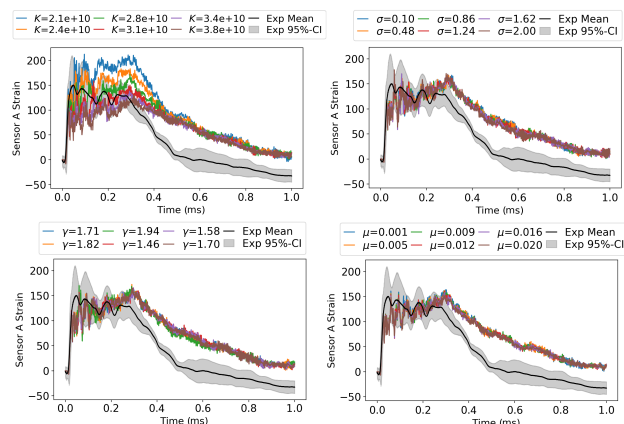


Figure 4: Effect of the four physical parameters on the sensor A strain: bulk modulus ( $K$ ), surface tension ( $\sigma$ ), adiabatic index ( $\gamma$ ), and viscosity ( $\mu$ ).

## Best Case Results

In this paper, we investigated more than 150 simulation cases, and each simulation takes an average of 20 hours on 256 Intel Xeon 2.30 GHz CPUs. The best simulation that matches the measured data is plotted in Fig. 5, which corresponds to  $K = 3.45e+10$  Pa,  $\sigma = 0.47$  N/m,  $\gamma = 1.66$ ,  $\mu = 0.0015$  N·s/m<sup>2</sup>, and 8 bubble families with bubble distribution 1 (Fig. 2, left). The results show that the best case captures sensors C, D, and E quite well, which is the same for sensors A, N, and P, but only for the beginning of the pulse. The simulation tends to overestimate the strain response after 0.4 ms, especially for sensors A and N. Current fatigue analysis of the target design focuses on the damage from strain range magnitude and does not account for the time required for these ranges. Therefore, the overestimated tail strain from the best case should have limited impact on the evaluation of the target's fatigue lifetime. The tail

strain discrepancy is also expected to be reduced, if not totally removed, by exploring a wider parameter space in the future.

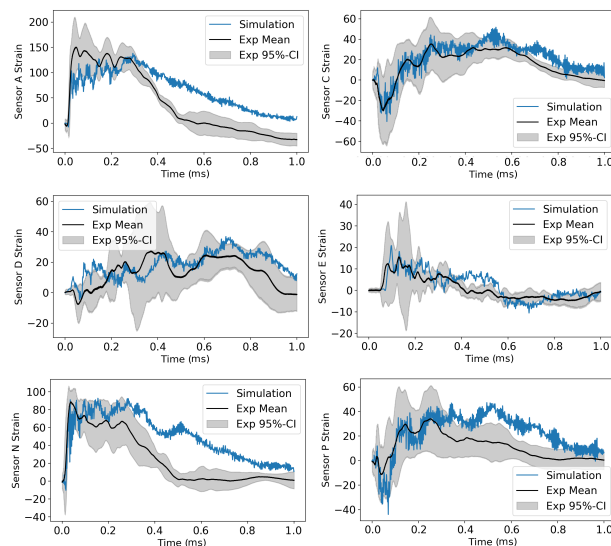


Figure 5: Simulated versus measured strain for various sensors for the best R-P simulation case.

## CONCLUSIONS

In this work, we have presented a benchmarking study of the simulation for the liquid mercury target at the SNS using a proposed 2-phase mercury model that includes bubble dynamics. Our preliminary results indicate that 8-10 bubble families with a monotonic right-skewed distribution seem to provide the best agreement with the experimentally measured strain response with helium gas injection. In addition, the bulk modulus seems to have more impact on the simulated strain than surface tension, viscosity, and adiabatic index. Although our simulations seem to provide good agreement at the beginning of the pulse, a consistent overestimation was seen toward the end of the pulse for some sensors.

Given the results achieved in this study by manual tuning and sensitivity analysis, the next step for the team is to expand their previously developed surrogate-based tuning methods based on neural networks and polynomial expansions [14], as well as Bayesian uncertainty quantification [13], for a more thorough analysis of the R-P model. These methods require accurate surrogate models to be trained, which implies more computing power is needed to execute the simulations to train the surrogates.

## REFERENCES

- [1] T.E. Mason, D. Abernathy, I. Anderson, J. Ankner, T. Egami, G. Ehlers, A. Ekkebus, G. Granroth, M. Hagen, K. Herwig, *et al.*, "The spallation neutron source in Oak Ridge: A powerful tool for materials research", *Physica B*, vol. 385, p. 955–960, 2006. doi:10.1016/j.physb.2006.05.281

- [2] Y. Liu, W. Blokland, C. Long, S. Murray, B. Riemer, R. Sangrey, M. Wendel, and D. Winder, “Strain measurement in the recent SNS mercury target with gas injection”, *J. Phys. Conf. Ser.*, vol. 1067, p. 052022, 2018. doi:10.1088/1742-6596/1067/5/052022
- [3] D.A. McClintock, B.W. Riemer, P.D. Ferguson, A.J. Carroll, and M.J. Dayton, “Initial observations of cavitation-induced erosion of liquid metal spallation target vessels at the Spallation Neutron Source”, *J. Nucl. Mater.*, vol. 431, p. 147, 2012. doi:10.1016/j.jnucmat.2011.11.021
- [4] Justin Mach, Kevin Johns, Sarma Gorti, and Hao Jiang, “Fatigue analysis of the spallation neutron source 2 MW target design”, *Nucl. Instrum. Methods Phys. Res., Sect. A*, vol. 1010, p. 165481 2021. doi:10.1016/j.nima.2021.165481
- [5] B.W. Riemer, “Benchmarking dynamic strain predictions of pulsed mercury spallation target vessel”, *J. Nucl. Mater.*, vol. 343, pp. 81–91, 2005. doi:10.1016/j.jnucmat.2005.01.026
- [6] L. Lin, S. Gorti, J. Mach, H. Tran, and D.E. Winder, “Application of Machine Learning to Predict the Response of the Liquid Mercury Target at the Spallation Neutron Source” Oak Ridge National Laboratory (ORNL), Oak Ridge, TN, USA, 2021. <https://www.osti.gov/biblio/1846539/>
- [7] D.A. McClintock, Y. Liu, D.R. Bruce, D. Winder, R.G. Schwartz, M. Kyte, W. Blokland, R.L. Sangrey, T.M. Carroll, C.D. Long, H. Jiang, and B.W. Riemer, “Small-bubble gas injection to mitigate cavitation-induced erosion damage and reduce strain in target vessels at the spallation neutron source”, *Mater. Des.*, vol. 221, p. 110937, 2022. doi:10.1016/j.matdes.2022.110937
- [8] K. Kikuchi, H. Kogawa, M. Futakawa, S. Ishikura, M. Kamimaga, and R. Hino. “R&D on mercury target pitting issue”, *J. Nucl. Mater.*, vol. 318, pp. 84–91, 2003. doi:10.1016/S0022-3115(03)00016-3
- [9] M. Futakawa, T. Naoe, C.C. Tsai, H. Kogawa, S. Ishikura, Y. Ikeda, H. Soyama, and H. Date, “Pitting damage by pressure waves in a mercury target”, *J. Nucl. Mater.*, vol. 343, pp. 70-80, 2005. doi:10.1016/j.jnucmat.2004.07.063
- [10] M. Futakawa and N. Tanaka, “Cavitation in High-power Pulsed Spallation Neutron Sources”, *Konsoryu*, vol. 24, p. 138, 2010. doi:10.3811/jjmf.24.138
- [11] D. Winder, L. Lin, and J. Mach, “Incorporating bubble growth volume feedback to improve simulation of the response of a structure containing liquid and gas to sudden energy input”, *Nucl. Instrum. Methods Phys. Res., Sect. A*, vol. 1005, p. 165371, 2021. doi:10.1016/j.nima.2021.165371
- [12] M.S. Plesset and A. Prosperetti, “Bubble dynamics and cavitation”, *Annu. Rev. Fluid Mech.*, vol. 9, p. 145-185, 1977.
- [13] M.I. Radaideh, L. Lin, H. Jiang, and S. Cousineau, “Bayesian inverse uncertainty quantification of the physical model parameters for the spallation neutron source first target station”, *Results Phys.*, vol. 36, p. 105414, 2022. doi:10.1016/j.rinp.2022.105414
- [14] M.I. Radaideh, H. Tran H, L. Lin, H. Jiang, D. Winder, S. Gorti, G. Zhang, J. Mach, and S. Cousineau, “Model calibration of the liquid mercury spallation target using evolutionary neural networks and sparse polynomial expansions”, *Nucl. Instrum. Methods Phys. Res., Sect. B*, vol. 525, pp. 41–54, 2022. doi:10.1016/j.nimb.2022.06.001